Performance Degradation of Grid-Tied Photovoltaic Modules in a Desert Climatic Condition

by

Adam Alfred Suleske

A Thesis Presented in Partial Fulfillment
of the Requirements for the Degree
Master of Science in Technology

Approved November 2010 by
The Graduate Supervisory Committee:

Govindasamy TamizhMani, Chair
Bradley Rogers
Narciso Macia

ARIZONA STATE UNIVERSITY

December 2010

ABSTRACT

Photovoltaic (PV) modules appear to have three classifications of failure: Infant mortality, normal-life failure, and end-of-life failure. Little is known of the end-of-life failures experienced by PV modules due to their inherent longevity. Accelerated Life Testing (ALT) has been at the crux of this lifespan prediction; however, without naturally failing modules an accurate acceleration factor cannot be determined for use in ALT. By observing modules that have been aged in the field, a comparison can be made with modules undergoing accelerated testing.

In this study an investigation on about 1900 aged (10-17 years) grid-tied PV modules installed in the desert climatic condition of Arizona was undertaken. The investigation was comprised of a check sheet that documented any visual defects and their severity, infrared (IR) scanning, and current-voltage (I-V) curve measurements. After data was collected on modules, an analysis was performed to classify the failure modes and to determine the annual performance degradation rates.

DEDICATION

I would like to dedicate this work to my grandmother, Gloria Pleasant.

Without her constant love and support this would not have been possible.

ACKNOWLEDGMENTS

I would first like to thank Dr. Govindasamy Tamizh-Mani for his guidance in my time studying at Arizona State University. I will forever be grateful for his guidance and for giving me the opportunity to work on a project of such importance. I would also like to thank Dr. Bradley B. Rogers and Dr. Narciso F. Macia for their interest and careful reading of this work.

I would also like to thank Arizona Public Service and the great people at the APS Solar Testing and Research facility. Their patience and help was invaluable—it was wonderful working with you.

I must also give great thanks to Lynette Salik at APS STAR. If it were not for her help on all of those 117°F days, this would never have been possible—I am forever indebted.

Finally, I must thank my family and my sweetheart, Sue. Every time I fall off the horse, you help me back up.

TABLE OF CONTENTS

Page

Page

Page

LIST OF TABLES

Table Page

LIST OF FIGURES

Figure Page

Figure Page

CHAPTER 1

Introduction

1.1 Background

Photovoltaic (PV) modules have an inherent longevity due to the materials used in their construction. Modern polymers and construction techniques have corrected the faults of the past; however, because these polymers are so new, little is known about their lifetime performance.

Attempts have been made to model the reliability of PV modules over the years. Accelerated testing has been heavily relied upon to create these models but without real-world data to compare results against a clear correlation cannot be determined. With modules in the field reaching 17+ years of age, data can now be collected to better understand PV reliability.

With an abundance of real world data available, the time to study PV reliability is now. This study was conducted to gain information about the aging of fielded PV modules so that reliability models can be developed and a deeper understanding of how they fail can be gained.

1.2 Statement of Problem

The purpose of this study was to determine the overall reliability and degradation of c-Si photovoltaic modules when fielded in desert Phoenix, AZ climatic conditions.

The knowledge gained from this study will benefit the photovoltaic (PV) community in several ways:

- PV manufacturers will have the ability to understand field issues and reduce the warranty returns
- PV consumers will gain confidence on the product durability and reliability
- Researchers will be able to develop physical and reliability models in conjunction with an accelerated lifetime testing.

The specific objectives of this study were to:

- Investigate crystalline silicon PV modules fielded at Arizona Public Service (APS) Solar Testing and Research (STAR) facility
- Identify modules with significant visual failures via a detailed visual inspection.
- Perform IR scanning on all the visually inspected modules
- Measure I-V curves of a set of visually failed and healthy modules
- Compare the performance data of visually failed and healthy modules with nameplate ratings
- Determine annual degradation rate for each module type

1.3 Scope

The scope of this study is shown in Figure 1. This study investigated the reliability of photovoltaic modules when fielded in Phoenix Arizona climatic conditions. Arizona Public Service (APS) Solar Testing and Research (STAR) facility was chosen for this investigation due to the age of modules being employed. The failure modes of the modules were observed and infrared (IR) screening was performed. Next, current-voltage (I-V) curves were taken of any modules showing a hot spot or non-uniform heat signature. I-V curves were also taken of a sample of modules that were found to not have any visible failures to serve as a sample for observing the health of the overall sample. Based upon the plate ratings on the back of the PV modules, degradation rates have been calculated.

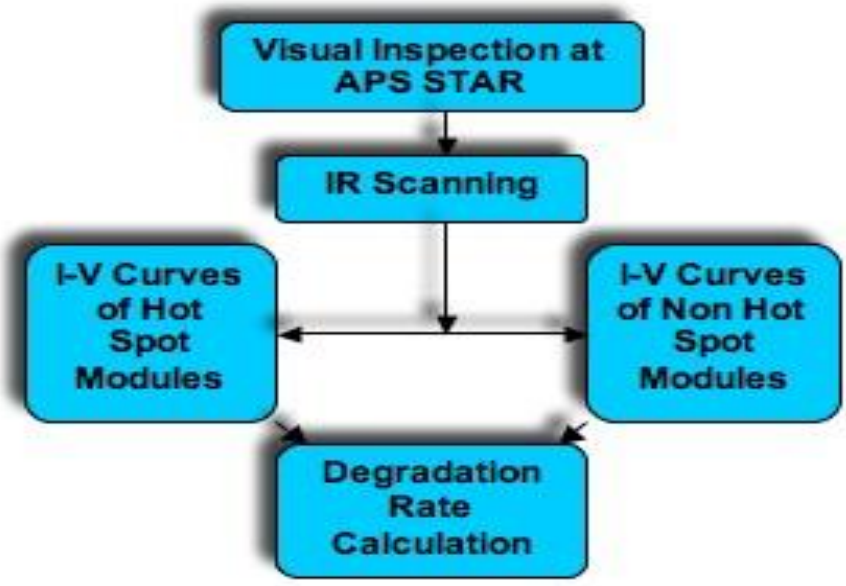

Figure 1. Scope flow chart of this study

CHAPTER 2

Literature Review

2.1 Reliability and Lifetime Prediction

The objective of this work was to determine the reliability of crystalline silicon (c-Si) photovoltaic (PV) modules in Phoenix Arizona climatic conditions. The reliability and lifespan of c-Si modules depends heavily upon module construction and the climate in which it is installed [5]. In this chapter a literature search related to the degradation of c-Si PV modules and the different module construction technologies are explained.

2.2 Why it is Necessary to Study Reliability

It has been well documented that photovoltaic modules are the most reliable component in a PV system [14]. Because of their long life span and low failure rate little information is known about how they fail, when they do. Understanding the failure mechanisms behind PV modules will lead not only to better warranties and longer service periods, but it will increase the safety of PV systems [12]. Little is known about the end-of-life for a PV module. A major concern is that they will loose their dielectric properties and become a fire hazard when functioning in high voltage systems [14].

Another benefit to studying the reliability of photovoltaics is the ability to warranty the amount of energy that modules will produce over its lifetime [11]. Seeing as how the lifetime of modules is finite, the amount of

energy that they can produce over that lifetime is finite as well. Being able to accurately predict the energy produced will add another cost point for consumers of PV modules.

2.3 Reliability Modeling

Real world data must be present to understand PV reliability. Statistically speaking, if one is to model a function against time, the only results that can be assumed acceptable are the ones that lead up to the current time; future predictions can be extrapolated however they can not be considered statically correct [10]. In the case of photovoltaic reliability, modules have not been fielded long enough to act as a measure of the accuracy of reliability models.

This study was preformed to collect the data necessary for reliability modeling. The modules involved range in age from 10 to 17 years old. The information collected allows for a new step to be taken towards the prediction of catastrophic failures and power production. This study also took into account the construction of the modules themselves to offer predictions based upon different module construction methods and materials—not only one blanket prediction.

2.4 Photovoltaic Degradation

Degradation of photovoltaic modules is assumed to be linear [11]; however the probability of failure is not. The failure rates can be charted and is known as the bathtub curve. This can be seen in Figure 2.

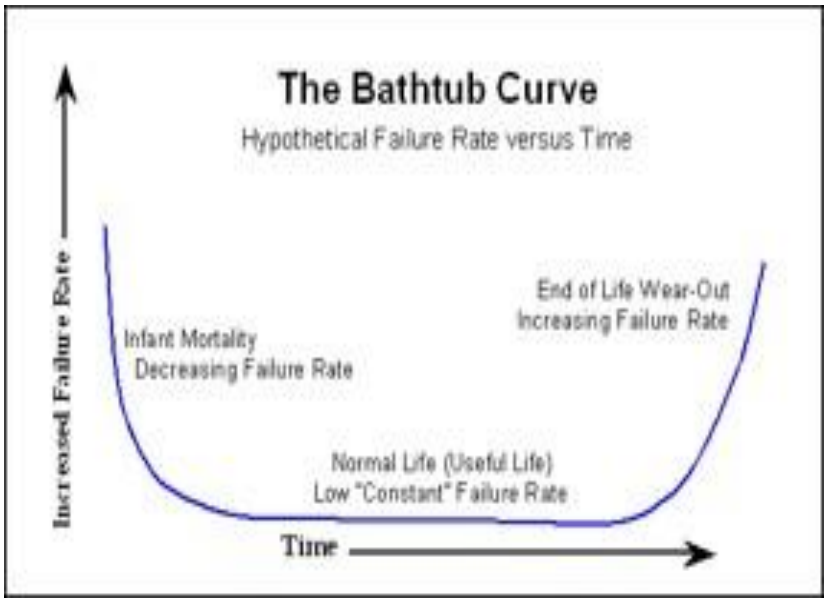

Figure 2. Bathtub curve of PV failure rates [10]

Initial failures are known as “infant mortality” failures and are associated with poor design and manufacturing defects. This portion of the curve is very well understood and will no longer be of discussion in this paper.

The middle section of the curve is known as “useful life.” This section shows that very few failures take place however those that do are typically catastrophic and are more concentrated near the end of the curve. This final section is known as “end-of-life.”

At the end-of-life, the rate of catastrophic failures increases. However, because of industry definition, modules that fail to produce 80% of original power are categorized to have reached their end-of- life as well.

2.4.1 Photovoltaic Useful Life

Useful life of PV modules is essentially determined by the user, however manufacturers define useful life by the warranty given to their product. The majority of manufacturers will promise no more than a 20% loss in power over the life of the warranty [10]. For the purpose of this study, useful life will be defined as a properly functioning module free from mechanical or cosmetic defects with less than 20% of original output power lost to date. The loss in power can be determined using the following formula (2.1).

$$P_{loss} = P_0 - P_t \quad (2.1)$$

Where:

P_{loss}: Power lost since original fielding

P_0: Power of module when originally fielded, taken from nameplate

P_t: Power of module at current time

2.4.2 Catastrophic Failure

Catastrophic failure is defined as any failure causing a photovoltaic module to suddenly perform more than 20% below the rated performance or cause a sudden mechanical or cosmetic failure. Severe thermal hot spotting, glass breakage, cell breakage, and burns in the substrate are a few examples of catastrophic failure [3, 6, 13].

2.5 Analysis

The analysis of PV modules in this study covered the failure modes and possible mechanisms involved. A series of steps were taken to determine the overall functionality of the modules to determine modules that are in the “useful life” stage and “end-of-life” stages of the bathtub curve.

2.5.1 Photovoltaic Failure Modes

Photovoltaic modules fail in many ways [3, 13]. The most common failure modes are corrosion, cell or interconnect breakage, output lead problems, junction box problems, delamination, hot spotting, and yellowing or browning of encapsulant [13, 14]. Examples of some of these failures can be seen Figures 3 through 6 below.

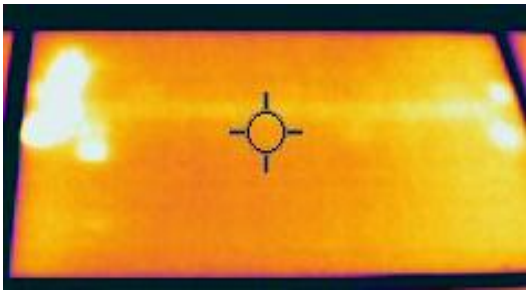

Figure 3. IR image of module hot spot

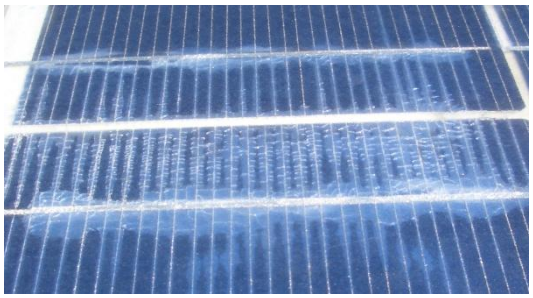

Figure 4. Delamination of encapsulant

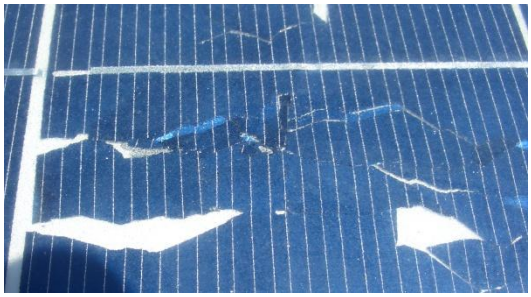

Figure 5. Shattered c-Si cell

Figure 6. Browning of cell center

Information on these failure modes was collected using a check sheet for each module in this study (Appendix A). The check sheet also covers a much wider variety of failures than those listed above however all failure modes may not be known until further study.

2.5.2 Causes of Photovoltaic Failure

The most common causes of failure in PV modules are known to be moisture penetration and temperature fluctuation [11, 13, 14]. In the general study of PV reliability, three areas of the United States are targeted for their climatic conditions: Colorado—cold and humid, Florida—hot and humid, Arizona—hot and dry. In the case of this study moisture penetration was extremely low due to the desert climate.

2.5.3 Infrared Scanning

Infrared scanning is a well-accepted method of module failure detection [3, 6, 13]. Infrared cameras work by detecting heat given off by the module it is pointed at and it displays the image as a color gradient on the screen. This allows for the temperature of all points of the module to be seen at once. It has proven effective in the detection of hot spots and cell-interconnect failures [3, 6, 12].

2.5.4 Dangers from Failing Modules

As modules age, a concern is that they may loose their dielectric properties and leak electric current [5]. This leakage of current can cause

a scenario known as DC arcing. The biggest concern with DC arcing is that once an electric arc is started it will not stop until it burns through the material that the arc is between. If not found in time DC arcing can be extremely dangerous and in some instances can cause fires. Part of this study will look into the instances where DC arcing has happened in the field over the lifespan of the modules.

The loss of dielectric properties is not the only cause of DC arcing. Broken interconnects between cells can also establish the conditions necessary for a DC arc to form [13]. Images of DC arcing can be referenced in Figures 7 and 8.

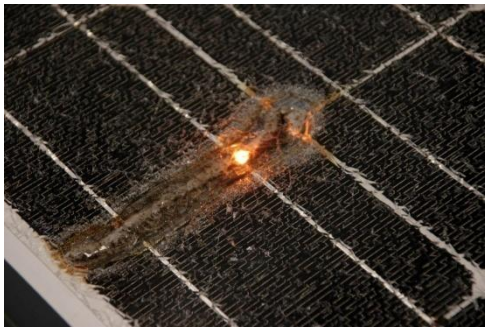

Figure 7. DC arc under superstrate [12]

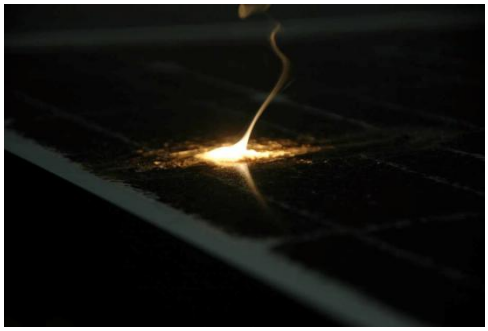

Figure 8. DC arc burning through superstrate [12]

2.6 Module Construction

The materials used in construction of PV modules are chosen based upon their ability to protect the silicon cells and connections without inhibiting their ability to produce power [5, 14]. The components associated with module robustness are the glass superstrate, encapsulating material, and the substrate [5].

2.6.1 Glass Superstrate

The glass superstrate used in c-Si module construction is typically tempered. This provides strength as well as high permeability to light by passing nearly 96% of the spectrum above 400 nm [7]. The glass can also be infused with the element Cerium to prevent excessive ultraviolet light penetration that in turn prevents deterioration of the encapsulating material [5, 13].

2.6.2 Encapsulating Material

Encapsulating materials are designed to provide protection for the c-Si cells needed to make PV modules. They can be made from different blends of polymers with the most popular formulation being ethyl vinyl acetate or EVA [5]. Encapsulants are all blended to be dielectric, impermeable to water, have high light transmittance, long lasting and soft for cell protection [5].

2.6.3 Backsheet

Backsheet materials are the final layer in PV module construction. The purpose of this layer is to protect the contents of the module from abrasion and moisture [4, 5]. Today many companies have moved away from glass substrates to polymer backsheet materials [4]. This switch has reduced the cost of the modules as well as the weight. Weight reduction has made for easier shipping and installation. Due to the nature of

polymer backsheets however, they are prone to moisture penetration after extended use [5].

In some cases glass substrates are still in use. A portion of the modules in this study had glass superstrates and substrates. The use of glass makes it very hard for moisture to penetrate the encapsulant. In the case of these modules the only entry point for moisture is through the edges of the module, which are sealed and framed.

CHAPTER 3

Methodology

3.1 Building a Failure Mode Database

The methodology for this PV module reliability prediction was based upon the collection of field data from a group of 1,865 modules fielded for up to 17 years. Figures 9 through 14 show the photographs of module types/models involved in this study.

Figure 9. Photograph of OPV1A modules

Figure 10. Photograph of OPV1B modules

Figure 11. Photograph of OPV2A modules

Figure 12. Photograph of OPV2B Modules

Figure 13. Photograph of OPV2C modules

Figure 14. Photograph of OPV2D modules

The process to collect field data started off with the creation of a check-sheet to be used to collect data about failure modes observed at the APS STAR facility (Appendix A). About 35 failure modes on the check-sheet were determined after an extensive search on prior works done on photovoltaic failures. Once the observations were underway, if any new failure modes were encountered they were then added to the check-sheet or noted in a column marked “other.”

3.1.1 Scope of Methodology

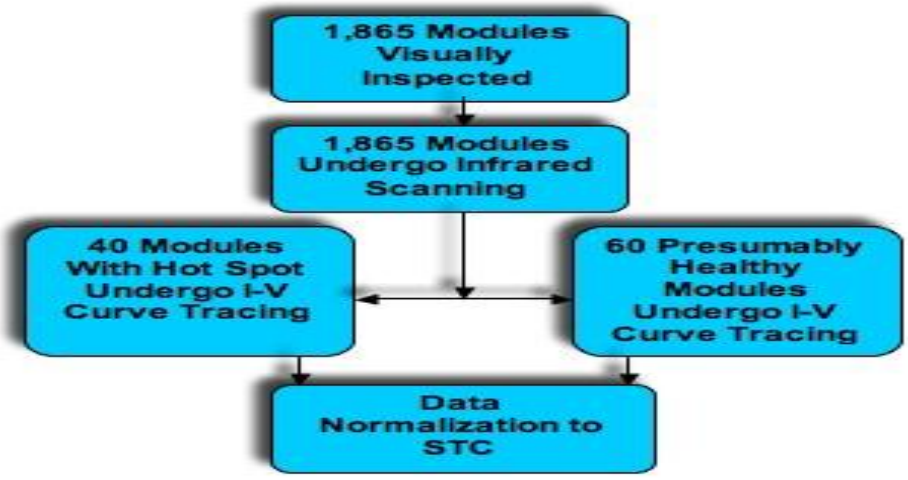

Figure 15. Scope of methodology flow chart

Figure 15 shows an outline of the methodology used in this study. The study started off with a visual inspection of 1,865 modules that was followed by an infrared scanning of the same modules. From the IR scanning, 40 hot spot modules were detected to undergo I-V curve tracing. 60 modules that were chosen at random and were presumably failure free (no hot spots or visual defects) also underwent I-V curve tracing. This data was then normalized to Standard Test Conditions (STC) for further analysis.

3.2 Visual Inspection

Based upon the terms defined by the PV industry, a PV module failure is considered anything cosmetic, mechanical, or performance affecting. For this study anything cosmetic or mechanically faulty was catalogued in a visual inspection of 1,865 modules. This would also prove to be the basis for predicting the difference in failures experienced by different module technologies and constructions.

3.3 Infrared Scan

To supplement the visual inspection and search for catastrophic failures, a FLIR I40 infrared camera was used to scan 1,865 modules. This scanning detected 40 modules exhibiting irregular heat signatures, also known as hot spots. In this study, a hot spot is defined as cell or group of cells that have a temperature difference greater than 5°C in relation to the rest of the module. The IR camera used had not been

calibrated so the temperature given was not accurate however the temperature gradients obtained were accurate. This was checked using two thermocouples to measure temperature difference between the hot spot and non hot spot. The Figure 16 is an example of one of the modules found to be containing a hot spot.

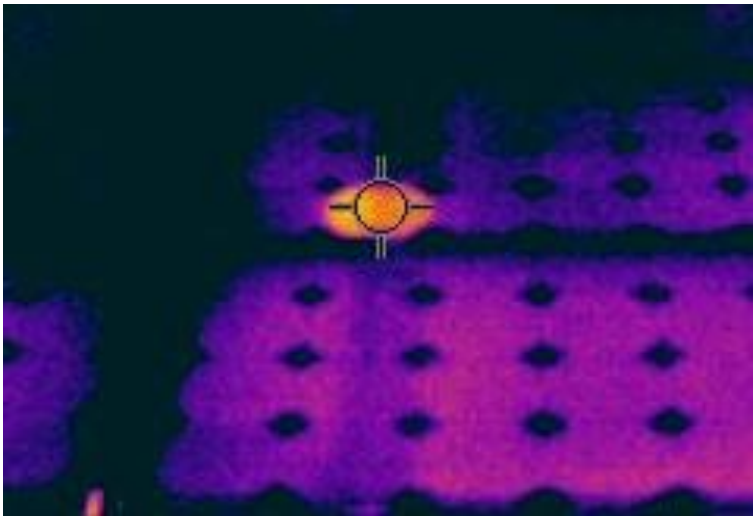

Figure 16. Infrared image of hot spot cell in module

When a module was found to have a hot spot it was considered a module of interest. This means that the module was determined to have catastrophically failed and would be subjected to further screening to observe the electrical characteristics.

3.4 I-V Curve Tracing

The next step in data collection was to take I-V curve traces of all 40 modules exhibiting hot spots. Before measurements were taken each module was washed to ensure that there was no shading due to soiling. This curve-tracing step determined whether or not the modules' electrical

characteristics were failing. Unfortunately, two modules could not have their electrical output measured. This was due to the fact that the junction boxes from the factory had been bypassed by the APS STAR facility and were hard-wired with no ability to disconnect those three modules from the string.

Curve tracing these modules showed in fact 100% of the modules exhibiting hot spots were failing electrically with abnormal curves and greatly reduced fill factors—some far below the power warranty given by manufacturers.

I-V curves of modules without hot spots were also taken. A random sampling of

10 modules from each model and manufacturer were selected for a total of 60 modules; presumably free from failure. Again these modules were washed before measurements were taken to eliminate shading.

3.4.1 Data Normalization

Due to the effects of temperature and irradiance on PV modules, data had to be normalized to standard test conditions. This step was performed using the ASTM-E1036-93 formulas (3.1) and (3.2).

$$I_0 = I + I[(E_0/E - 1) + a(T_0 - T)] \quad (3.1)$$

$$V_0 = V + b(T_0 - T) – (I – I_0)*R_s - K*I_0(T_0-T) \quad (3.2)$$

Where:

I = measured current, A

I_o = normalized current, A

I_{sc} = measured short-circuit current, A

E_o = irradiance at standard rated conditions (SRC), 1000 W/m^2

E= irradiance, W/m^2

V = measured voltage, V

V_o = normalized voltage, V

V_{oc} = measured open-circuit voltage, V

T_o = temperature at standard rated conditions, 25 °C

T = measured temperature, °C

a = temperature coefficient of device under test, 1/°C

b = temperature coefficient of device under test, V/°C

R_s = Series Resistance, Ohms

K = curve correction factor, Ohms/°C

Data was collected using a Daystar DS-100C I-V curve tracer. The irradiance was measured using technology-matched reference cells with thermocouples integrated into the cell. The ambient temperature was measured using a thermocouple onboard the curve tracer and finally the temperature of the module was measured using a thermocouple attached to the substrate of the module.

As shown in Figure 17, for the purpose of normalization, the series resistance was calculated by determining the slope of the I-V curve nearest to V_{oc}.

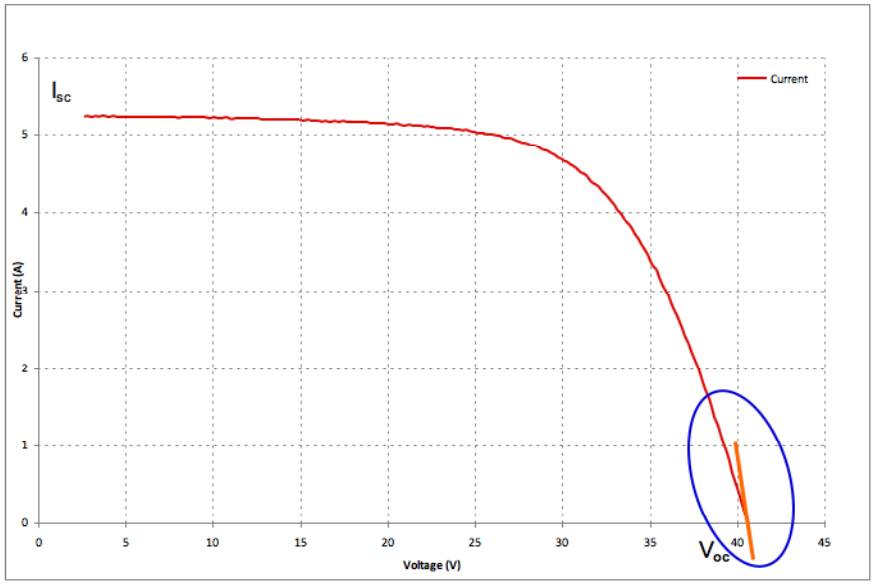

Figure 17. Series resistance approximation - orange line is the slope of curve near V_{oc}

The two temperature correction coefficients determine the change in current (I) and voltage (V) of the module depending upon operating temperature. These coefficients were collected from the specification sheets for each model of PV module.

To simplify normalization of data, IVPC Version 2.63 software was used. The software allowed all temperature constants to be entered in one screen and automatically calculate the series resistance. An example can be seen in Figure 18.

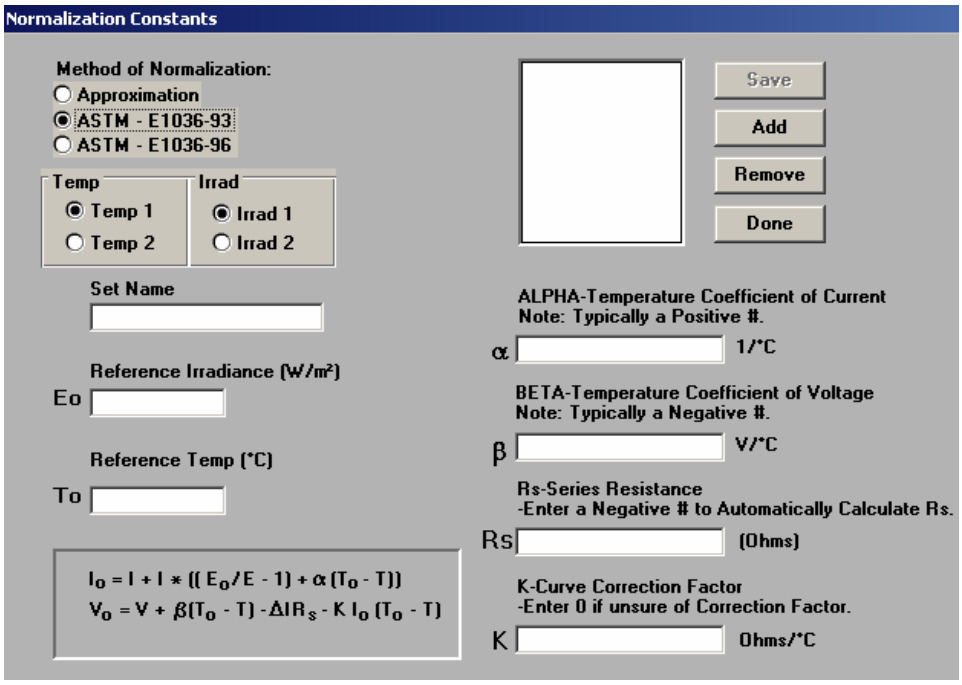

Figure 18. ASTM-E1036-93 normalization screenshot

The final step in data analysis requires the information gathered from I-V curves to be entered into Microsoft Excel 2004. Once imported, data analysis could be performed.

CHAPTER 4

Results and Discussion

4.1 Models and Module Count

This section will discuss the effects of weather and age on 6 different photovoltaic models from four manufacturers for a total of 1,865 modules. Table 1 shows the breakdown of module counts among 6 models leading to an overall installed capacity of about 190 kW.

Table 1. Model designation and module count

Array	Model A	Model B	Model C	Model D	Model E	Model F
Size	21.1 kW	81.9 kW	51.3 kW	12 kW	8.8 kW	14.4 kW
#Modules (1-axis)	168	1092	171	48	50	120
#Modules (Lat.Tilt)	216	-	-	-	-	-

The purpose of this work is not to rate the manufactures so the names corresponding to the models are not disclosed in the discussion. For the remainder of this paper, the modules will simply be referred to by Model A, B, C, D, E, and F. The arrays in which the modules are mounted and numbers of years, as of June 2010, the modules were fielded along with construction types are provided in Table 2 and Figure 19A.

Table 2. Photovoltaic module ages

Model A	Model B	Model C	Model D	Model E	Model F
455V DC*	455V DC*	400V DC*	400V DC*	445V DC*	430V DC*
Mono – Si	Mono – Si	Poly – Si	Poly – Si	Mono – Si	Poly - Si
Glass/Polymer	Glass/Polymer	Glass/Glass	Glass/Polymer	Glass/Polymer	Glass/Polymer
17 years	12.3 years	10.7 years	10.7 years	10.7 years	10.7 years

***Array open circuit voltage

4.2 Visual Inspection

The visual inspection provided immediate feedback about the predominate failures occurring in photovoltaic modules when fielded in Phoenix/Tempe, AZ climatic conditions. Despite the wide array of failure modes that have been documented in the field, there was only a limited number of failure modes found in this study. The occurrences of failures are shown below in Table 3.

Table 3: Types of module failures at ASP-STAR

Module	Module Count	Modules Affected
A – Mono-Si (17 years; glass/polymer)	384	
Browning in cell center	384	100.00%
Frame seal deterioration	384	100.00%
Hot spot (IR Scan)	4	1.0%
B – Mono-Si (12.3 years; glass/polymer)	1092	
Encapsulant delamination	2	0.2%
Browning in cell center	1092	100.0%
Hot spot (IR Scan)	2	0.6%
C – Poly-Si (10.7 years; glass/glass)	171	
Broken cells	47	27.5%
Encapsulant delamination	55	32.2%
Hot spot (IR Scan)	26	15.2%
White material near edge cells	2	1.2%
White material browning	56	32.8%
D – Poly-Si (10.7 years; glass/polymer)	48	
Browning in cell center	37	77.1%
Hot spot (IR Scan)	4	8.3%
E – Mono-Si (10.7 years; glass/polymer)	50	
Bubbling substrate	33	66.0%
Browned substrate near Jbox	50	100.0%
F – Poly-Si (10.7 years; glass/polymer)	120	
Discolored cell patches	6	5.0%
Backsheet bubbling	1	0.8%
Browned spots on backsheet	2	1.7%
Metallization discoloration	22	18.3%
Frame seal deterioration	15	12.5%
Hot spot (IR Scan)	4	3.3%
Total Modules:	**1865**	

The most predominant failures were cosmetic and were minor. Figure 19B below shows the percentage of each of the most predominate failure modes in the sample.

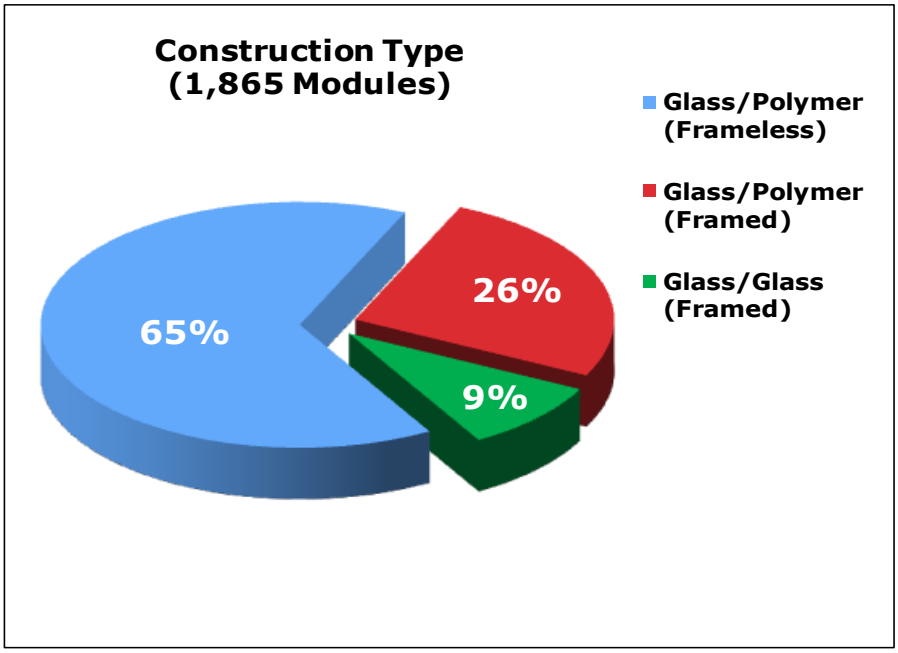

Figure 19. Construction types out of 1865 modules

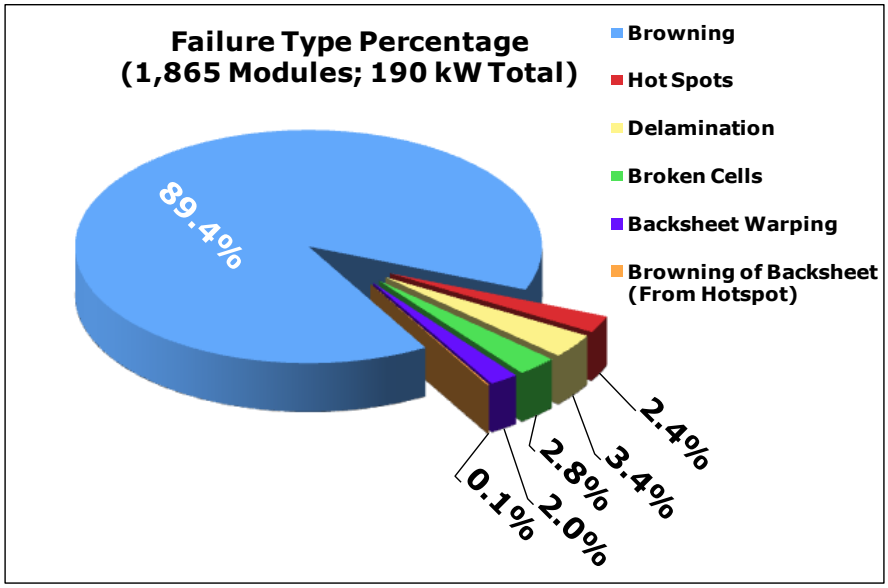

Figure 20. Failure type percentages out of 1,865 modules

Browning of the encapsulant near the center of the cell was the most widely observed failure type at 89.1%. Encapsulant browning can have an effect on the power output. Figures 21 through 23 show the encapsulant browning in the center of the cells in Module A, B, and C.

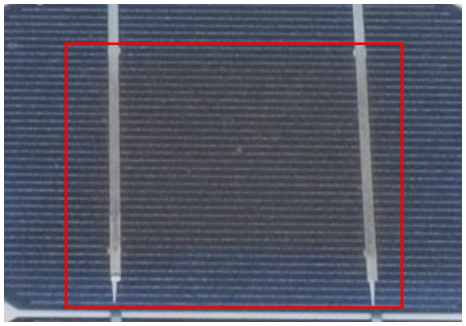

Figure 21. Module A cell center browning

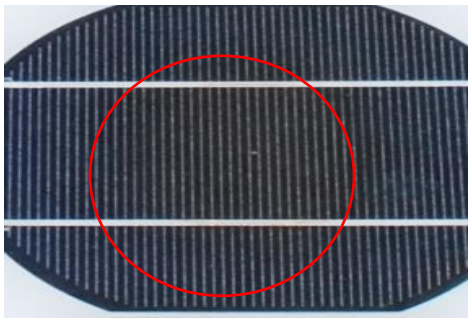

Figure 22. Module B cell center browning

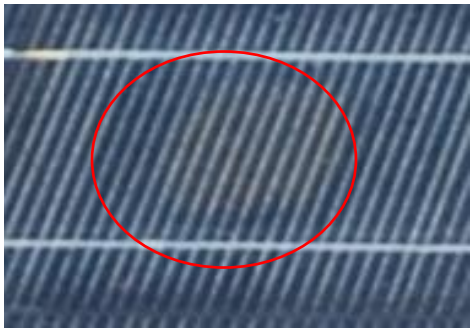

Figure 23. Module C cell center browning

There were many cases of delamination of the encapsulant; however, they were confined almost totally to Model C, glass/glass modules. Model B experienced 2 cases of delamination spread over 1092 modules, a total of 0.18%. Model C however experienced 55 cases of delamination out of a total of 171 modules for a total of 32.16%. Model B has been fielded about two years longer and experienced only a small

fraction of the delamination of Model C. Figures 24 and 25 show relative severity of delamination found in Models B and C. Another noteworthy point is that Model A has been fielded about seven years longer than Model C and has zero cases of delamination.

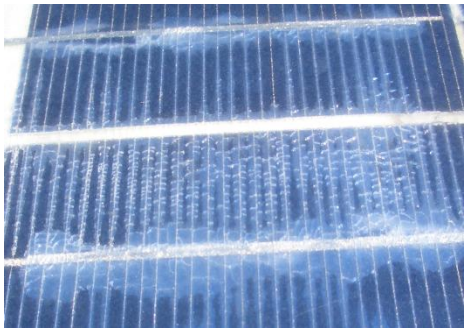

Figure 24. Model C Delamination

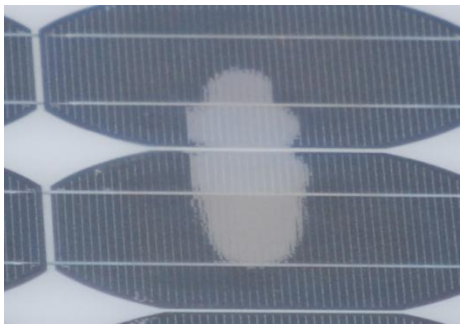

Figure 25. Model B Delamination

The occurrence of older modules having less delamination than newer modules is believed to be rooted in the construction. Polymer backsheets such as the ones used in Models A, B, D, E, and F are able to maintain lower module temperatures as well as the laminates are breathable leading to oxidative bleaching of encapsulants. This reduction in exposure to high temperatures and increase in breathability are believed to reduce the occurrences of encapsulant delamination.

Polymer backsheeting works well at reducing high operating temperatures; however, it can have some drawbacks when exposed to high temperature. Just as encapsulant delamination due to excessive heat, the polymer backsheet can delaminate or bubble. Models E and F showed instances of backsheet bubbling. Due to the brightness of the

white polymer backsheet, it was not possible to photograph this phenomenon—to draw a comparison; however, the effect is much like that of an air bubble being caught underneath a decal.

Some of the bubbles in the backsheet however had turned a light brown. This browning is probably caused by overheating due to a hot spot in the module. Again, this was unable to be photographed due to how light the discoloration was.

The most important finding in the visual inspection is not what was seen rather what was not seen. Out of the 1,865 modules observed there were no burns, no broken glass and no visible broken interconnects. This is important because it shows that the safety record of these modules appears to be very high and show no immediate danger of DC arcing or fire.

4.3 Infrared Scanning

The infrared (IR) scanning of all 1,865 modules was performed to evaluate the presence and severity of hot spots. IR scanning under grid-tied condition was performed over sunny days with approximately 1,000 W/m^2 of irradiance. Due to concerns with time, modules were not short circuited in this scan. Scanning showed that there were 40 hotspot modules in the sample yielding a total of 2.2%. Figure 26 shows the total percentage of hotspot modules by model.

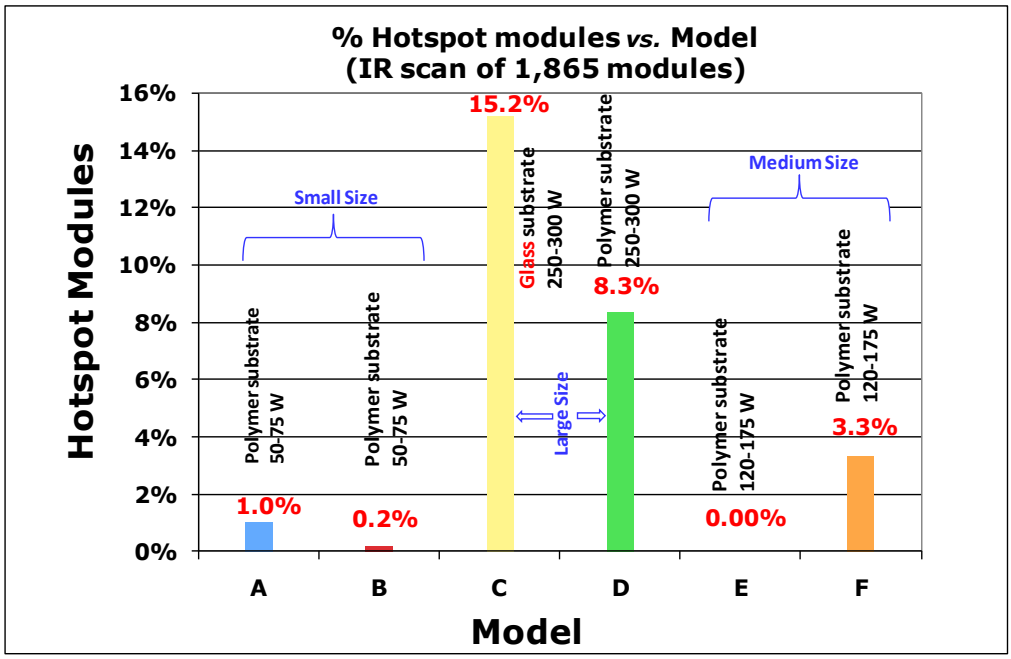

Figure 26. Breakdown of hotspot modules by model

(All are glass/polymer modules except "C" which are glass/glass modules)

It is immediately obvious that Model C has the highest percentage of hot spots. It is believed that the thermal stress of the glass/glass construction and large size could be primary causes for this failure type. The second highest percentage of hot spots is found in Model D. Model D was also made of large size modules. As expected, the large size modules are more susceptible to thermal expansion and contraction of cell components including interconnects, superstrate/substrate and frames. Higher thermal expansion and contraction is expected to lead to higher hotspot issues.

The worst hotspot found was on a Model C module and had a temperature difference of 25.8 °C between the surrounding cells and the hot spot cells. Figure 27 show an infrared image of the model with the

worst hot spot. The IR camera had not yet been calibrated; however, it was determined through a cross check with another thermal sensor that its scale was correct.

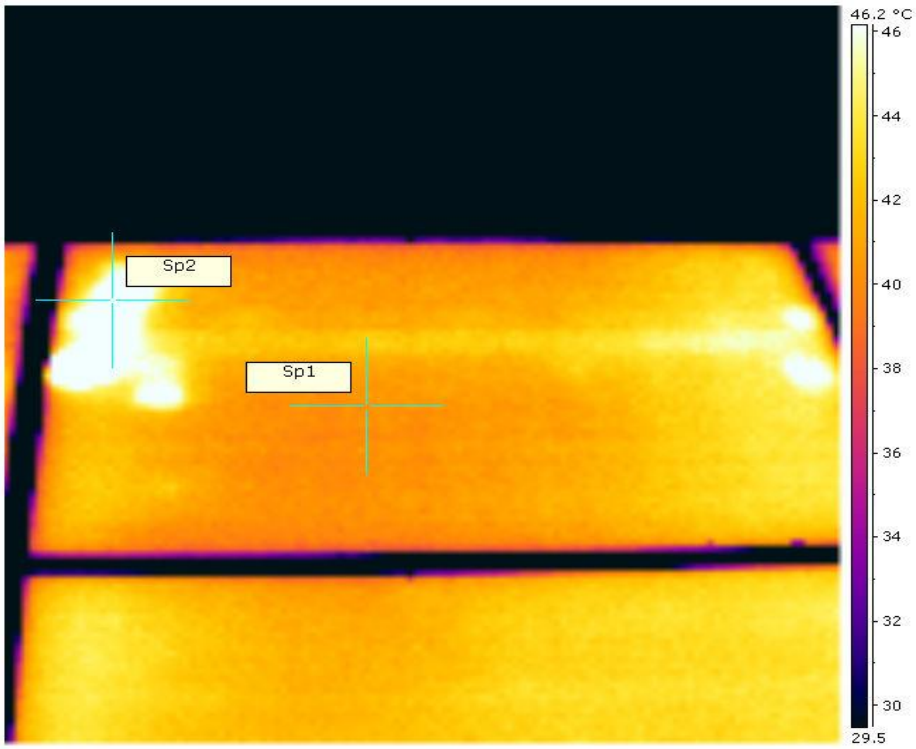

Figure 27. IR image of Model C - most severe hotspot in sample

In the Figure 27 above, Sp1 was found to be the lowest temperature of the entire module with a cell temperature of 40.4°C while Sp2 was found to be the highest temperature with a cell temperature of 66.2°C.

Matching the findings from the visual inspection, there were no failures so severe that became a safety issue. What IR scanning did provide was a very fast and easy way to locate failing modules that are performing far below the modules around it. This technique could be

employed to more quickly and easily find defective modules in a PV power plant that are decreasing the performance of an entire string or array.

4.4 Overall Power Degradation

I-V curve tracing provided several different results—some were surprising. The results of the hot spot modules showed that their curves were not normal and confirmed that many modules had their average power output had dropped below 20% of nameplate rating.

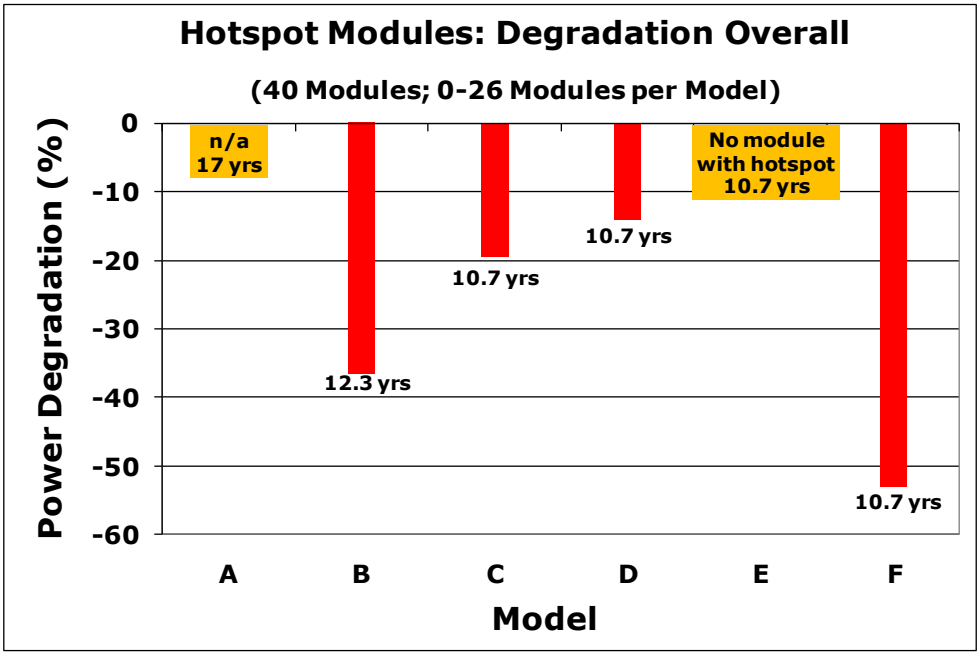

Figure 28. Degradation of hotspot modules (all years)

Figure 28 shows the average power drop from the nameplate rating of the models. There does not appear to be any discernable correlation between the age and extent of hotspots. The modules of Model C (10.7 years old) experienced about 15% (highest) hotspot occurrences and

about 19.5% power degradation whereas the modules of Model F (10.7 years old) experienced only about 3% hotspot occurrences but about 53% power degradation. This indicates that there is no direct correlation between hotspot severity, age, and power degradation unless the location/type of hotspot is sensitive to power generation issue (rather than safety issue). It seems that the hotspot modules of Model A are a special case. According to the data obtained from the I-V curve tracer, the power output of Model A had no power drop over the 17 years of fielding. Not knowing if it was human error during measurements by test personnel or labeling/binning (mixing higher power binned modules with lower power binned modules) by the manufacturer, it is felt that these findings deserve further attention and further study. These results will not be discussed in the remainder of this report.

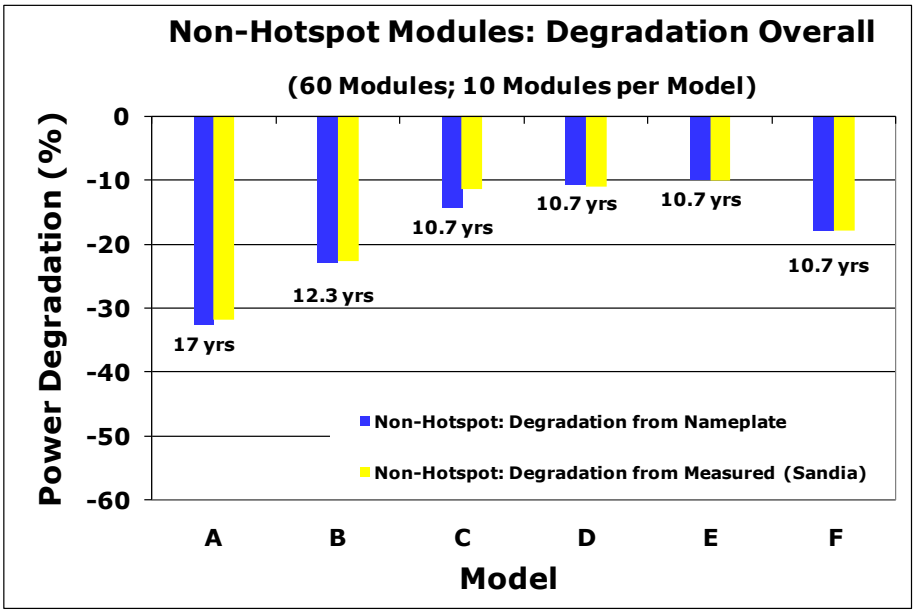

Figure 29. Degradation of non-hotspot modules (all years)

Figure 29 shows the average percent loss in power output of non-hotspot modules for each model in this study. For uniform comparison among the six models, all the modules considered in this performance degradation analysis were 1-axis tracker mounted modules excluding the fixed-tilt modules of Model A. All models had expected declines in power output, however, the magnitude of decline was surprisingly high. From this figure it becomes apparent that age is a primary factor in power loss amongst non-hotspot modules (about 98% of 1965 modules) – 12.3 and 17 years old modules, respectively, experienced about 23 and 33% power degradations; 10.7 years old modules experienced between 10 and 18% power degradations. From this figure, it is apparent that a large number of these fielded modules may not meet the commonly provided warranty requirements of less than 20% performance drop over 20-25 years. In the absence of initial performance data of all the modules tested in this project, the performance degradation calculations were performed assuming that the nameplate ratings of the manufacturers were accurate. In order to cross check if this assumption is valid, the performance degradations were calculated again with the data obtained from Sandia National Laboratories “Photovoltaic Module Database.” Sandia had, fortunately, independently measured and published the STC data of all these models and they were used in these calculations. As shown in

Figure 29, the manufacturer nameplate ratings are closely matching with Sandia's independent data. However, it is still assumed that the modules supplied to APS-STAR are of the same performance and design quality modules supplied to Sandia for independent measurements and open publications.

4.5 Annual Power Degradation

In the absence of intermittent performance data on the individual modules, the degradation rate of PV modules has been assumed to be linear. It is believed that as the module ages its annual degradation rate increases towards the end of its life. In Figure 29, one can see that the non-hotspot modules of older Models, A and B, have much higher annual degradation rates (1.9%) than that of the younger models C, D and E (1.3%). This could possibly imply that at some point during fielding the modules started aging at a more severe rate. However, the non-hotspot modules of Model F have degraded at much higher annual rate (1.7%) than its 10.7 years old counterparts (1.3%). This is possibly due to some design issues of Model F and these issues could be related to the inappropriate component selection, cell processing, cell interconnection and/or packaging. Table 4 shows degradation rates of each model by average percent drop per year. Again, one can observe that there is a noticeable increase in degradation rate between 10.7 years and the 12.3 or 17 years old modules. As discussed earlier, there does not appear to

be any direct correlation between annual power degradation and hot spot severity unless the hotspot location/type is sensitive to power generation (rather than safety). The modules of Model C experienced about 15% (highest) hotspot issues and only about 3% annual power degradation whereas the modules of Model F experienced only about 3% hotspot issues but about 5% annual power degradation. Also, power degradation rate of Model C (highest % of hotspot modules) increased from 1.3% for non-hotspot modules to only 1.8% for hotspot modules whereas the power degradation of Model F increased from 1.7% for non-hotspot modules to surprisingly 5% for hotspot modules. This indicates again that there is no direct correlation between the extent of hotspots and power degradation rate. It seems the location and type (low shunt or high shunt) of hotspots in Model C is less sensitive to power degradation as compared to the location/type of hotspots in Model F.

Table 4. Degradation rates by model

Model of Module	Years Fielded	% Degradation (Non-hotspot)	% Degradation/Year (Non-hotspot)
Model A	17 years	-32.57%	-1.92%
Model B	12.33 years	-22.97%	-1.86%
Model C	10.66 years	-14.27%	-1.34%
Model D	10.66 years	-10.53%	-0.99%
Model E	10.66 years	-9.94%	-0.93%
Model F	10.66 years	-17.9%	-1.68%

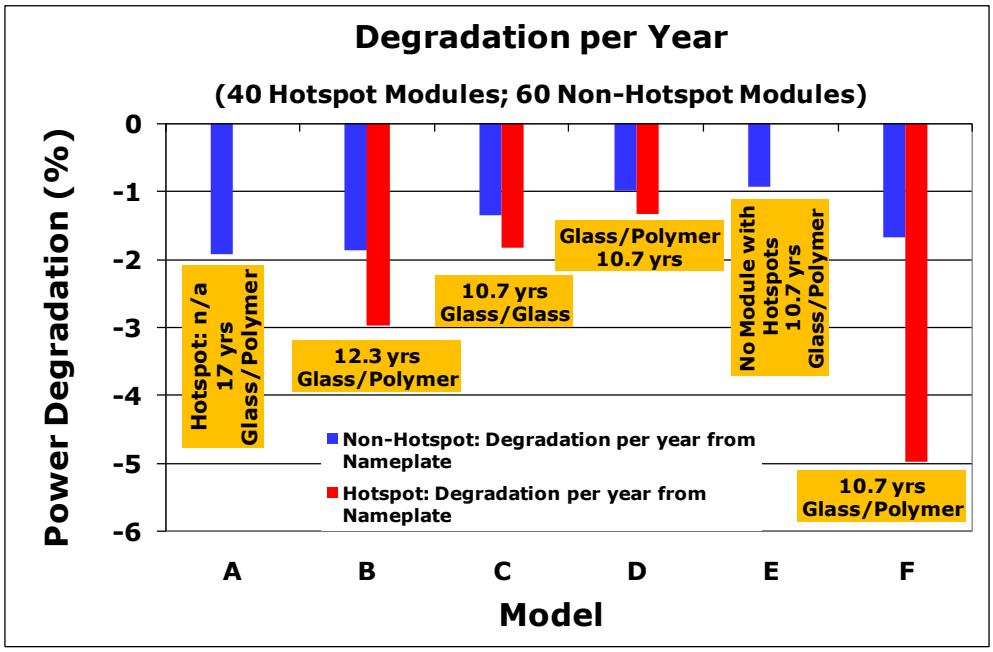

Figure 30. Degradation rate of hotspot and non-hotspot modules (per year)

To delve further into the annual degradation rates, one can notice that the annual degradation rates obtained in this study are higher than those previously reported. In a study performed by NREL [9] in Golden, Colorado, different modules were individually held at maximum power to study degradation. From the NREL and other module level long-term studies performed at ASU, it is seen that the crystalline silicon PV modules degrade at less than 0.5% per year. However, from the current study one could determine that c-Si modules degrade between -0.93% and -1.92% per year. This significant difference in degradation rate may lie in the system voltage levels, module mismatch and insolation levels (1-axis vs. fixed-tilt) of the systems investigated in this study.

The OPV 1 and OPV 2 systems consist of a large number of modules connected in series. This series connection brings about two possible issues for the increased degradation rate: a system voltage of 400V and module mismatch. When modules are connected in series they must all have equal current outputs, if not, a bottleneck effect can occur in the module with the least current output. This bottleneck effect causes the module to dissipate the backed up current as heat energy, degrading the module.

In regards to the high system voltage, the high voltage can reduce the effectiveness of the encapsulant dielectric properties allowing a slight leakage current between the cells and frame/grounding. This leakage current comes out of the photovoltaic cells causing an electrochemical corrosion of cell components (especially metallic components) at the interface between the cell and encapsulant. The electrochemical corrosion becomes photoelectrochemical corrosion in the presence of sunlight and it is known to be much worse than simple chemical or electrochemical corrosion. Neither (high voltage and mismatch) of these effects can take place unless the module is connected in series such as in the case of a system composed of large arrays studied in this project.

A study conducted by NREL [8] was found to have similar results as this investigation. In 2005, NREL obtained data showing that the grid-connected (approximately 10 years old; fixed tilt) high system voltage

based c-Si modules degraded between 0.9% and 1.3% per year. If one compares the results of NREL to the results of this study (0.93% to 1.68% degradation per year for 10.7 year old modules), it becomes apparent that system voltage and module mismatch over time could be the plausible explanation for a higher degradation rate of modules at the system level as compared to module level. It is to be noted that the insolation (1-axis) and temperature experienced by the grid-tied APS-STAR's modules are higher and hence the annual degradation rate is expected to be higher as compared to the NREL's grid-tied module.

CHAPTER 5

Conclusions and Recommendations

5.1 Conclusions

The conclusions drawn from the extensive analysis of field degraded modules is presented in this section. Due to the broadness of the topic, it was not possible to study all aspects of photovoltaic degradation; however, recommendations on future work are made in the next section.

5.1.1 Visual Failures

The visual failures observed in this study came with different variety and different severity. It is apparent that the browning of the encapsulant materials is the largest issue with the appearance or performance of PV modules. The next failure that draws interest is the case of hotspots. In this study, there was not always a visible explanation of the cause of hotspots. Without a visual indicator, it is assumed to be the case of cell mismatch and/or corrosion of metallization or solder bonds in the interconnects during the manufacturing or ageing process. It is also apparent that hot spots is not always dangerous scenario, however, it is power robbing. Modules with hotspots show drastic decreases in power over their non-hotspot counterparts. This can be detrimental in supplying power from a string or array. Just one hotspot module in a string will decrease the power of the entire string and therefore the array may not

meet power demands. Like stated earlier in this work, the most impressive finding is not what was seen as much as what was not seen. Out of the 1,865 modules visually inspected, there were no signs of broken interconnects, or burns in the backsheet materials. This finding is important for the public to understand because it will improve overall consumer confidence.

5.1.2 Module Construction

Difference in module construction did appear to have an effect on module performance. After observing the rates of delamination, it became apparent that excessive heating caused by glass/glass construction accelerates the delamination process. Again, seeing as how this study was conducted in a hot and dry climate, it is not to say that the glass/glass module construction would not succeed elsewhere. The glass/glass construction may prove an excellent choice in an area that is cooler or more humid. The impermeability of the glass substrate makes it an excellent choice for a moisture barrier but limits the ambient temperature in which it will uphold.

5.1.3 Power Degradation Rate

In this study, with the exception of Model F, it can be seen that as modules age the rate at which they degrade has an increase. The modules aged between 12.3 and 17 years degraded at about 1.9% per year. All the 10.7 years old modules degraded at 0.9-1.3% per year

except Model F which degraded at about 1.7% per year. The reason for the higher degradation rate of Model F modules could not be completely explained in this short-term non-destructive study; however, it could be possibly related to the design, process or component selection issues of the modules. The higher degradation rates of grid-tied PV modules as compared to individually exposed modules are attributed to the system voltage related corrosion, module mismatch and insolation levels.

5.2 Recommendations

Because of the breadth of the survey involved in this work, certain things were assumed for the sake of saving time. If this project were to be continued, it is recommended that the temperature coefficients be measured in the field rather than taken from specification sheets. In furthering the study of hotspot issues, it is suggested using an infrared camera that has been recently calibrated so that the temperature reading is accurate and not just the temperature gradient. The gradient is a strong tool to measure; however, the actual temperatures may provide more useful information when attempting to predict where phenomenon such as DC arcing may occur. It is also suggested to conduct further performance and labeling related investigation into the hotspot modules of Model A. Most importantly, it is suggested that this study be repeated at least once a year for the next 5-10 years so the end of life failure modes and mechanisms can be determined.

REFERENCES

1) M. J. Cushing, "Another Perspective on Temperature Dependence of Microelectronic-Device Reliability," *MIL-HDBK-217*, 1993.

2) W. Gambogi, E. McCord, H. Senigo, S. Peacock, and K. Stika, "Failure Analysis Methods Apllied to PV Module Reliability," 2009.

3) J. Granata, W. Boyson, J. Kratochvil, and M. Quintana, "Long-term Performance and Reliability Assessment of 8 PV Arrays at Sandia National Laboratories," *Photovoltaic Specialists Conference*, 2009.

4) G. Jorgensen, K. Terwilliger, S. Glick, J. Pern, and T. McMahon, National Center for Photovoltaics and Solar Program Review Meeting, Topic: "Materials Testing for PV Module Encapsulation," CO, 2003.

5) M. Kempe, DOE Solar Energy Technologies, Topic: "Module Encapsulant Diagnostic and Modeling," CO, 2005.

6) D. King, J. Kratochvil, M. Quintana, and T. McMahon,"Applications for Infrared Imaging Equipment in Photovoltaic Cell, Module, and System Testing," 2008.

7) D. King, J. Kratochvil, M. Quintana, D.E. Ellibee, and B.R. Hansen, "Photovoltaic Module Performance and Durability Following Long-term Field Exposure," *Progress in Photovoltaics: Research and Applications*, 2000.

8) B. Marion, J. Adelstein, K. Boyle, H. Hayden, B. Hammond, T. Fletcher, B. Canada, D. Narang, D. Shugar, H. Wenger, A. Kimber, L. Mitchell, G. Rich, and T. Townsend. "Performance Parameters for Grid-Connected, 2006.

9) C. Osterwald, R., J. Adelstein, J.A Del Cueto, B. Kroposki, D. Trudell, and T. Moriarty. "Comparison of Degradation Rates of Individual Modules Held at Maximum Power." 2006.

10) Photovoltaic Reliability Class, Topic: “Failure Rates and the Bathtub Curve.” AZ, 2009

11) M. Vasquez and I. Ray-Stolle, "Photovoltaic Module Reliability Model

Based on Field Degradation Studies," *Progress in Photovoltaics: Research and Applications*, 2008.

12) W. Vaaßen and J. Zornikau, International Workshop , Topic: "Failure Mechanism of Contact Faults in the DC- Circuit of the PV Arrays," Burgdorf. Oct. 2007.

13) J. Wohlgemuth, NREL Reliability Workshop , Topic: "Failure Modes of Crystalline Si Modules," CO, Feb. 2010.

14) J. Wohlgemuth, NCPV and Solar Program Review Meeting, Topic: "Long Term Photovoltaic Module Reliability." CO, 2003.

APPENDIX A

CHECKSHEET TEMPLATE FOR FIELD DATA COLLECTION

Reliability Checklist: Visual and Other Non-Destructive Inspections

Model Number
Serial number
Broken/chipped cells
Delamination
Bubbles
Discoloration of encapsulant
Cracked edges of encapsulation
Cell discoloration
Broken interconnect
Solder bond failure
Output lead problem
Cable deterioration
Connector deterioration
Substrate (backsheet) warping/detaching
Substrate (backsheet) cracking/crumbling
Burn through backsheet
Frame corrosion/rust
Broken glass
Frame joint separation
Frame cracking
Metallization discoloration
Seal deterioration
Solder melted
Hot spot on solder tabs / bus bars
Hot spot on cells
Junction box arcing
Junction box cracking
Junction box adhesive failure
Zero Isc
Open circuit
Low Isc
Cell mismatch
Low Pmax
Erratic I-V data
Infrared scan
Electroluminescence scan
Other (specify)
Other (specify)
Other (specify)